Novel mapping in non-equilibrium stochastic processes

Heseltine, J. & Kim, E. J.

Original citation & hyperlink:
Heseltine, J & Kim, EJ 2016, 'Novel mapping in non-equilibrium stochastic processes' Journal of Physics A: Mathematical and Theoretical, vol. 49, no. 17, 175002.
https://dx.doi.org/10.1088/1751-8113/49/17/175002

DOI 10.1088/1751-8113/49/17/175002
ISSN 1751-8113
ESSN 1751-8121

Publisher: IOP Publishing

Novel mapping in non-equilibrium stochastic processes

James Heseltine, Eun-jin Kim

School of Mathematics and Statistics,

University of Sheffield, Sheffield, S3 7RH, U.K.

Abstract

We investigate the time-evolution of a non-equilibrium system in view of the change in information and provide a novel mapping relation which quantifies the change in information far from equilibrium and the proximity of a non-equilibrium state to the attractor. Specifically, we utilize a nonlinear stochastic model where the stochastic noise plays the role of incoherent regulation of the dynamical variable x and analytically compute the rate of change in information (information velocity) from the time-dependent probability distribution function. From this, we quantify the total change in information in terms of information length $\mathcal{L}$ and the associated action $\mathcal{J}$ where $\mathcal{L}$ represents the distance that the system travels in the fluctuation-based, statistical metric space parameterized by time. As the initial PDF's mean postion (μ) is decreased from the final equilibrium value μ_* (the carrying capacity), $\mathcal{L}$ and $\mathcal{J}$ increase monotonically with interesting power-law mapping relations. In comparison, as μ is increased from μ_*, $\mathcal{L}$ and $\mathcal{J}$ increase slowly until they level off to a constant value. This manifests the proximity of the state for large $\mu > \mu_*$ and its stronger correlation to the attractor. Our proposed mapping relation provides a new way of understanding the progression of the complexity in non-equilibrium system in view of information change and the structure of underlying attractor.

I. INTRODUCTION

Many systems in nature or laboratories are nonlinear and involve stochastic processes due to intrinsic variability, heterogeneity, or uncertainty in a system [1–8]. An interesting consequence of the complex interaction in these nonlinear systems is the ability to self-regulate [1, 2, 9], leading to the formation of an attractor; a set of states, invariant under the dynamics, towards which neighboring trajectories asymptotically approach following the dynamical evolution. In understanding the time-evolution of a system far from equilibrium, one of the main challenges is the computation of the probability density function (PDF), in particular, its time-evolution, due to the probabilistic nature of the system (e.g. see [1, 2]). Unlike in equilibrium, there no longer exists a reservoir which maintains the system at certain temperature with constant fluctuations in the system. In fact, far from equilibrium, the level of fluctuations in the system changes with time and becomes a dynamical variable itself, and the importance of a full knowledge of the evolution of PDFs cannot be overemphasized. As the computation of time-dependent PDFs is highly demanding and expensive numerically, in this paper, we utilize one analytically solvable nonlinear stochastic system and investigate the time-evolution of this system from the point of the information change.

In equilibrium, thermodynamics can be endowed with a geometric structure (e.g. see [10–13]). For instance, [10] related the second moment of flutuations to the inverse of a metric tensor as neighboring points are well correlated through fluctuations. Of notable applications of a fluctuation-based metric are the comparsion of two equilibrium states via a statistical distance, or the interpretation of the interaction in a system via the curvature of the metric tensor (e.g. near phase transition). Similar metric structure was also utilized in quantum systems [13–15]. Generalization of this concept to a non-equilibrium system was attempted by different authors although they tend to be limited to the analysis of systems not far from equilibrium [12, 16–18]. Most recent effort includes the utilization of this concept in controlling a system to minimise entropy production, or even the experimental measurement of the statistical distance to validate a theory [12, 19–21]. By generalizing this concept to far-from equilibrium, [22, 23] we highlight physical implications of the metric for the structure of the attractor and the information flow by devising information length $\mathcal{L}$ and action $\mathcal{J}$.

The purpose of this paper is to utilize information length $\mathcal{L}$ and action $\mathcal{J}$ in an analytically solvable nonlinear stochastic model to understand the behavior of our system around its attractor. We present a novel mapping between the non-equilibrium state and the distance to the attractor through $\mathcal{L}$ and use $\mathcal{J}$ to describe the energy contained in the information. The remainder of this paper is organized as follows. In §II, we provide the formulation of our model. §III presents our motivation and derivation of $\mathcal{L}$ and $\mathcal{J}$. Our results and conclusions are provided in §IV and §V, respectively.

II. FORMULATION OF THE PROBLEMS

Our model is based on the logistic-type equation where the nonlinear negative feedback contains a stochastic random component [7] given in the following form:

$$\frac{dx}{dt} = \gamma x - (\epsilon + \xi) x^2 \tag{1}$$

Here $x \geq 0$ is a non-negative random variable of interest; the terms involving $\gamma > 0$ and $\epsilon > 0$ represent linear postive and nonlinear negative feedbacks, respectively, and ξ is the stochastic random part of the negative feedback, which is taken to have a short correlation time given by:

$$\langle \xi(t)\xi(t')\rangle = 2D\delta(t-t'), \tag{2}$$

and zero mean value $\langle \xi(t)\rangle = 0$; D is the strength of the stochastic forcing and angular brackets $\langle\rangle$ in Eq. (2) denote average over ξ. The solution to Eq. (1) is found as

$$\frac{1}{x} = \frac{1}{x(0)} e^{-\gamma t} + \frac{\epsilon}{\gamma}(1 - e^{-\gamma t}) + \int_0^t e^{-\gamma(t-t_1)} \xi(t_1) dt_1, \tag{3}$$

where $x(0) \equiv x_0$ is the value of x at $t = 0$ and $\Gamma = \int_0^t e^{-\gamma(t-t_1)}\xi(t_1)dt_1$ is a random, Gaussian process. For a fixed x_0, as in the case of the initial distribution given by a delta function centered around x_0, we can find the transition probability between the initial state $x(t=0) = x_0$ at $t = 0$ and the state $x(t)$ at time t by utilizing the Gaussian property of Γ as $P(\Gamma) = \sqrt{\frac{\beta}{\pi}} e^{-\beta\Gamma^2}$ for appropriate inverse temperature β which is completely determined by its first moment ($\langle\Gamma\rangle = 0$) and second moment. Specifically, the second moment is related to β as $\langle\Gamma^2\rangle = \frac{1}{2\beta}$ where the inverse temperature β is given by

$$\beta(t) = \frac{\gamma}{2D(1 - e^{-2\gamma t})}. \tag{4}$$

The transition PDF is then obtained through the conservation of probability,

$$P(x,t;x_0,0) = \frac{1}{x^2}\sqrt{\frac{\beta}{\pi}}e^{-\beta(\frac{1}{x}-A)^2}, \tag{5}$$

where $A = \frac{e^{-\gamma t}}{x_0} + \frac{\epsilon}{\gamma}(1-e^{-\gamma t})$, $x_0 = x(t=0)$. It is useful to note that as t tends to infinity, A tends to $\mu_* = \frac{\epsilon}{\gamma}$, the carrying capacity of the system, around which the PDF will be centered in the long time limit. To consider a more general case of an initial PDF with a finite width, we assume $1/x_0 = y_0$ to be a random Gaussian variable with a mean value $1/\mu$ and a finite variance $1/\beta_0$, the initial PDF is given by $P(y_0,0) = y_0^2\sqrt{\frac{\beta_0}{\pi}}e^{-\beta_0(y_0-\frac{1}{\mu})^2}$. The PDF $P(x,t)$ can then be shown as [26]:

$$P(x,t) = \frac{1}{x^2}\sqrt{\frac{\beta_1}{\pi}}e^{-\beta_1(\frac{1}{x}-A_\mu)^2}, \tag{6}$$

where

$$A_\mu = \frac{e^{-\gamma t}}{\mu} + \frac{\epsilon}{\gamma}(1-e^{-\gamma t}), \quad \beta_1(t) = \frac{\beta_0\beta(t)}{e^{-2\gamma t}\beta(t)+\beta_0}. \tag{7}$$

From Eqs. (4) and (7), we observe that as $t \to \infty$, $\beta_1 \to \gamma/2D \equiv \beta_*$, the inverse temperature of the final equilibrium PDF.

III. INFORMATION LENGTH $\mathcal{L}$ AND ACTION $\mathcal{J}$

When trying to understand non-equilibrium systems, the temporal variation in the PDF is of main importance. Due to the conservation of total probability, the integral of $\frac{\partial P(x,t)}{\partial t}$ over all states is equal to zero. Thus we quantify the change in information through the fluctuating energy, using the second moment of $\frac{\partial P(x,t)}{\partial t}$, given by

$$v^2(t) = \int \frac{1}{P}\left(\frac{\partial P}{\partial t}\right)^2 dx. \tag{8}$$

Here, $v(t)$ in Eq. (8) is the information velocity, which quantifies the rate at which the (dimensionless) information changes. This also defines a characteristic, dynamical time-scale for the evolution (the time unit), $\tau(t) = \frac{1}{v(t)}$. The total accumulated information change in an interval $[t_i, t_f]$, where t_i and t_f are the initial and final times, respectively, is obtained from the total elapse of the time measured in unit of τ(t) as

$$\mathcal{L}(t) = \int_{t_i}^{t_f}\frac{dt}{\tau(t)} = \int_{t_i}^{t_f}\left[\sqrt{\int\frac{1}{P}\left(\frac{\partial P}{\partial t}\right)^2 dx}\right]dt, \tag{9}$$

which is called the information length. Eq. (9) provides total change in information across the interval and is the total distance between the initial and final PDFs in statistical space. Also associated with information, we can quantify the energy content of the information by $v^2(t)$ and action $\mathcal{J}$

$$\mathcal{J}(t) = \int_{t_i}^{t_f} v^2(t)dt = \int_{t_i}^{t_f} \left[\int \frac{1}{P} \left(\frac{\partial P}{\partial t} \right)^2 dx \right] dt. \tag{10}$$

Note that we call $\mathcal{L}$ and $\mathcal{J}$ the information length and action, respectively (instead of thermodynamic length and divergence) to highlight their non-equilibrium nature [22, 23].

By using Eq. (6), we can compute Eq. (8) as

$$v^2(t) = \frac{\dot{\beta_1}^2}{2\beta_1^2} + 2\beta_1 \dot{A_\mu}^2, \tag{11}$$

where $\dot{\beta_1}$ and $\dot{A_\mu}$ are the time derivatives of β_1 and A_μ in Eq. (7). Computing these functions and substituting them into Eq. (11), we obtain

$$v^2(t) = \frac{2\gamma^2}{T^2}(r^2 + qT), \tag{12}$$

where $q = \frac{\beta_0}{\gamma}(\epsilon - \frac{\gamma}{\mu})^2$, $r = 2\beta_0 D - \gamma$, and $T = 2\beta_0 D(e^{2\gamma t} - 1) + \gamma$. We note that q (r) represent the difference in the mean value (variance) of x between the initial and final times.

By using Eq. (12) in Eqs. (9) and (10), we can calculate $\mathcal{L}$ and $\mathcal{J}$, respectively. First, the computation of $\mathcal{J}$ is straightforward:

$$\begin{aligned} \mathcal{J} &= \int_{T_i}^{T_f} \left\{ \frac{\gamma}{T^2} \frac{1}{T + r}(r^2 + qT) \right\} dT \\ &= \gamma \left[-\frac{r}{T} + \left(\frac{q}{r} - 1 \right) \ln \left(\frac{T}{T + r} \right) \right]_{T_i}^{T_f}, \end{aligned} \tag{13}$$

where T_i and T_f are T evaluated at t_i and t_f respectively. Next, to compute $\mathcal{L}$

$$\mathcal{L} = \frac{1}{\sqrt{2}} \int_{T_i}^{T_f} \left\{ \frac{1}{T} \frac{1}{T + r} \sqrt{r^2 + qT} \right\} dT, \tag{14}$$

we let $y = \sqrt{r^2 + qT}$ to recast Eq. (14) as

$$\begin{aligned} \mathcal{L} &= \frac{\sqrt{2}}{r} \int_{y_i}^{y_f} \left\{ \frac{r^2}{y^2 - r^2} + \frac{qr - r^2}{y^2 + qr - r^2} \right\} dy \\ &= \frac{1}{\sqrt{2}} \left[\ln \left(\frac{y - r}{y + r} \right) \right]_{y_i}^{y_f} + \frac{\sqrt{2}}{r} H, \end{aligned} \tag{15}$$

where y_i and y_f are y evaluated at T_i and T_f, and H is defined as

$$H = \int_{y_i}^{y_f} \frac{qr - r^2}{y^2 + qr - r^2} dy. \tag{16}$$

Eq. (16) is to be evaluated seperately for two cases: $q \geq r$ and $q < r$. First, for $q \geq r$, we use $y = \sqrt{qr - r^2}\tan\theta$ in Eq. (16) to obtain

$$H = \sqrt{qr - r^2} \int \frac{\sec^2\theta}{\tan^2\theta + 1} d\theta \tag{17}$$

$$= \sqrt{qr - r^2} \left[\tan^{-1}\left(\frac{y}{\sqrt{qr - r^2}} \right) \right]_{y_i}^{y_f}. \tag{18}$$

Secondly, in the $q < r$ case, we let $y = \sqrt{|qr - r^2|}\sec\theta = \sqrt{r^2 - qr}\sec\theta$ ($\cos\theta = \frac{\sqrt{r^2 - qr}}{y}$) to obtain

$$H = -\sqrt{r^2 - qr} \int \frac{1}{\sin\theta} d\theta$$

$$= -\frac{\sqrt{r^2 - qr}}{2} \left[\ln\left(\frac{y - \sqrt{r^2 - qr}}{y + \sqrt{r^2 - qr}} \right) \right]_{y_i}^{y_f}. \tag{19}$$

We note that Eq. (16) is continuous across $q = r$. In summary, Eq. (15), (18) and (19) give the information length Eq. (15) where $H = \sqrt{qr - r^2}\tan^{-1}\left(\frac{y}{\sqrt{qr - r^2}} \right)$ (for $q \geq r$) or $-\frac{\sqrt{r^2 - rq}}{2} \ln\left(\frac{y - \sqrt{r^2 - rq}}{y + \sqrt{r^2 - rq}} \right)$ (for $q < r$). For $\mu = \mu_* = \frac{\gamma}{\epsilon}$ ($q = 0$), we obtain $\mathcal{L}$ directly from Eq. (14) as follows:

$$\mathcal{L} = \frac{1}{\sqrt{2}} \int_{T_i}^{T_f} \left\{ \frac{1}{T} \frac{1}{T + r} |r| \right\} dT = \frac{1}{\sqrt{2}} \frac{|r|}{r} \ln\left[\frac{T}{T + r} \right]. \tag{20}$$

which gives a continuous mapping when paired with Eq. (20).

Finally, it is useful to examine the bahavior of $\mathcal{L}$ and $\mathcal{J}$ in the limit of $r = 0$ where the initial and final PDFs have the same width. By setting $r = 0$ in Eqs. (13) and (14), we obtain

$$\mathcal{J} = \int_{T_i}^{T_f} \frac{\gamma q}{T^2} dT = -\gamma q \left[\frac{1}{T} \right]_{T_i}^{T_f}, \tag{21}$$

$$\mathcal{L} = \frac{1}{\sqrt{2}} \int_{T_i}^{T_f} \frac{\sqrt{q}}{T^{\frac{3}{2}}} dT = -\sqrt{2q} \left[\frac{1}{\sqrt{T}} \right]_{T_i}^{T_f}. \tag{22}$$

IV. DEPENDENCE OF $\mathcal{L}$ AND $\mathcal{J}$ ON β_0 AND μ

As t and x can always be scaled by γ and ϵ, respectively, only two out of the four parameters γ, ϵ, D (or β_*), and β_0 are independent. Therefore, in the remainder of this paper, we fix $\mu_* = \gamma/\epsilon = 2$ and $\beta_* = 100 = \gamma/2D$ ($D = 0.01$, $\gamma = 2$, $\epsilon = 1$) and vary the initial PDF mean position (μ) and inverse temperature (β_0). To introduce the mapping between information change and the initial distance from the attractor and physical meaning, we start by examining how the PDF evolves in t and x and for different μ and $1/\beta_0$ of the initial PDF. We then examine how $\mathcal{L}$ and $\mathcal{J}$ depend on t, μ and β_0.

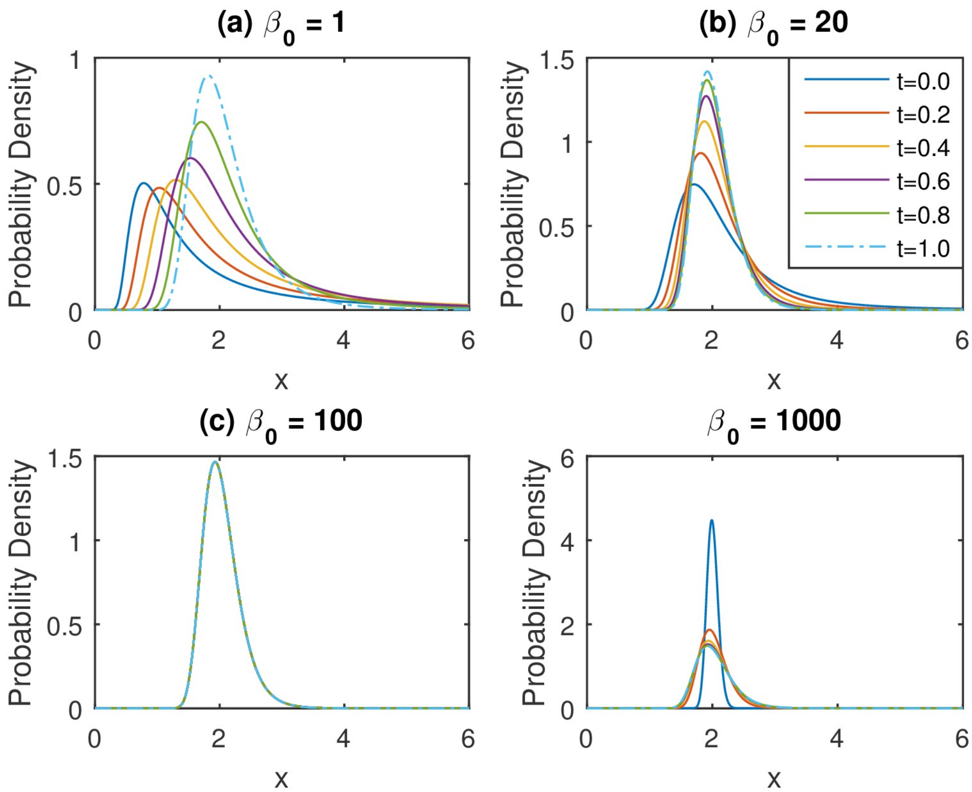

FIG. 1: PDFs against x shown at different t: $\beta_0 = 1, 20, 100, 1000$ in (a)-(d): $\beta_* = 100$

First, in Fig. 1, we fix $\mu = \mu_*$ ($q = 0$) and show PDFs against x for different initial inverse temperature $\beta_0 = 1, 20, 100, 1000$ in panels (a)-(d). Panels (a) and (b) are the cases where $\beta_0 < \beta_*$ while Panel (d) is the opposite case $\beta_0 > \beta_*$. Panel (c) corresponds to the special case of $r = 0$ where $\beta_0 = \beta_*$, demonstrating no change of the PDF in time. This is simply because the initial state is already in equilibrium, undergoing no further change in the PDF in time. No change in the PDF is then translated into no change in information content. That is, since the initial and final states are the same states and contain the same amount of information, the distance between these two states is zero in statistical space (see $\mathcal{L} = 0$ and $\mathcal{J} = 0$ at $\mu = 2$ in Fig. 5(c)).

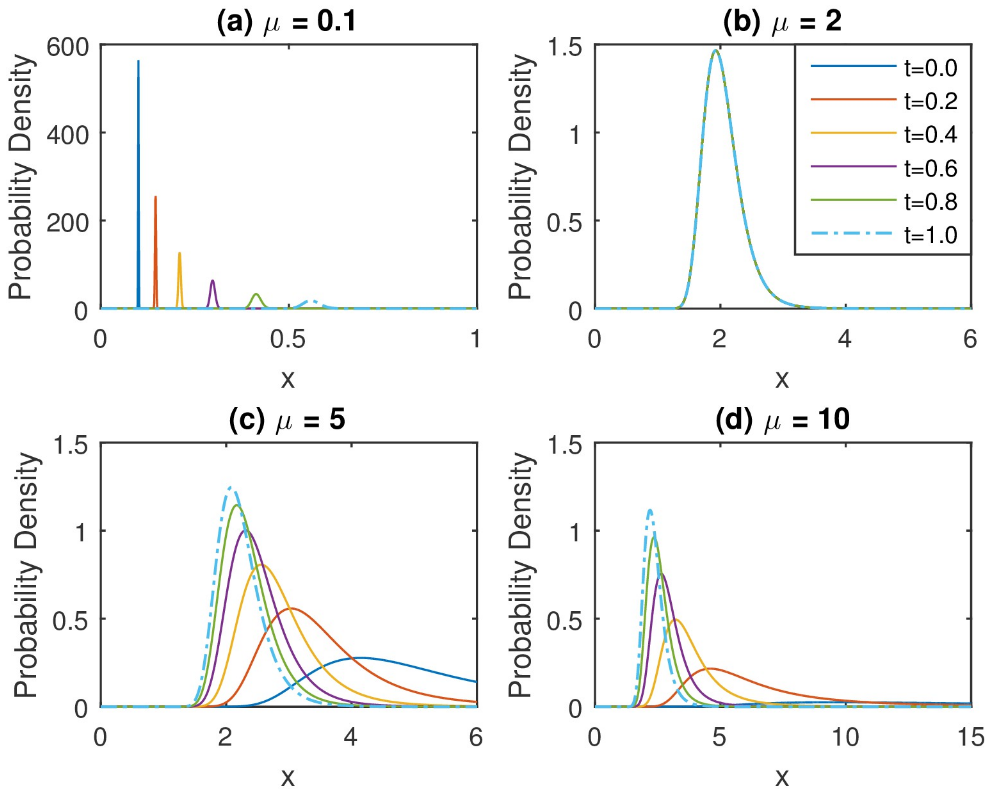

FIG. 2: PDF against x shown at different t for $\beta_0 = 100 = \beta_*$: $\mu = 0.1, 2, 5, 100$ in (a)-(d).

To complement Fig. 1, we fix $\beta_0 = \beta_* = 100$ ($r = 0$) and show PDFs against x for $\mu = 0.1, 2, 5, 100$ in Fig. 2 (a)-(d). For the larger $\mu > \mu_*$ ($= 2$) in Fig. 2(d), shifting the PDF seems to occur more rapidly towards equilibrium than shifting of the peak starting at $\mu < \mu_*$ towards μ in Fig. 2(a). The movement of the PDF peak at $\mu > \mu_*$ however takes place with much overlap with PDFs at consequent times, in contrast to the shifting of PDFs at $\mu < \mu_*$ where the overlap between PDFs at different times is insignificant. As a result, the total change of PDFs (information velocity) tends to be larger at $\mu < \mu_*$, compared to that at $\mu > \mu_*$. It is useful to note that the narrow width and large height of the initial peaks in panel (a) is because β_0 is defined for $y = x^{-1}$. Since $\mu = 0.1$ in panel (a), the peak lies within $[0, 1]$ thus the scaling within this region causes peaks closer to the origin to become narrower. To show this clearly, we obtain peak position $x_p = {y_p}^{-1}$ of the PDF from $\frac{dP(x,0)}{dx} = 0 = \frac{dy}{dx}\frac{d}{dy}[y^2 e^{-\beta_0(y-y_0)^2}]$ as $y_p = 0.5\left[y_0 + \sqrt{y_0^2 + 4{\beta_0}^{-1}}\right]$ ($y_0 = \mu^{-1}$), and thus $y_p \sim y_0$ (for large β_0) and $P(y_p) \sim P(y_0) = y_0^2 = \mu^{-2} \gg 1$ for $\mu \sim 0.1$. The width of

$P(x,0)$, corresponding to the width of $P(y,0)$, say $dy = \frac{1}{\sqrt{\beta_0}}$ follows from $dy = d\left(\frac{1}{x}\right) = \frac{-dx}{x^2}$ as $|dx| = |dy|x^2 = \frac{\mu^2}{\sqrt{\beta_0}} = \frac{0.01}{10} = 0.001$ for $\mu = 0.1$ and $\beta_0 = 100$.

In Figs. 3 and 4, we use $\beta_0 = 99$ and $\beta_* = 100$ (near $r = 0$) and show $\mathcal{L}$ and $\mathcal{J}$ against μ for different t. The sharp troughs visible in both Figs. 3 and 4, showing a huge drop in the information change around μ_*, are due to our (intentional) choice of $\beta_0 \simeq \beta_* = \gamma/2D$ (corresponding to $r \simeq 0$). That is, as $\beta_0 \sim \beta_*$, the initial variance being very close to the variance of the equilibrium state, only a very small change in the information occurs in reaching the equilibrium. We observe in Fig. 3 that information length increases much more significantly as μ moves away from the carrying capacity μ_* toward zero, and interestingly, this increase is found to obey a power-law (see below for this). In comparison, as μ is increased from μ_*, $\mathcal{L}$ and $\mathcal{J}$ increase slowly until they level off to a constant value. This manifests the proximity of the state and the stronger correlation to the attractor, as μ increases from the carrying capacity.

In order to show the robustness of our results, we consider different values of $\beta_0 = 20, 99, 100, 1000$, including $\beta_0 = 99$ in Fig. 3 to help comparison, in Fig. 5 (a)-(d). Moving from panels (a) to (d), β_0 increases. In Panel (c), $\mathcal{L} = 0$ at $\mu = \mu_*$ (see Eq. (21)

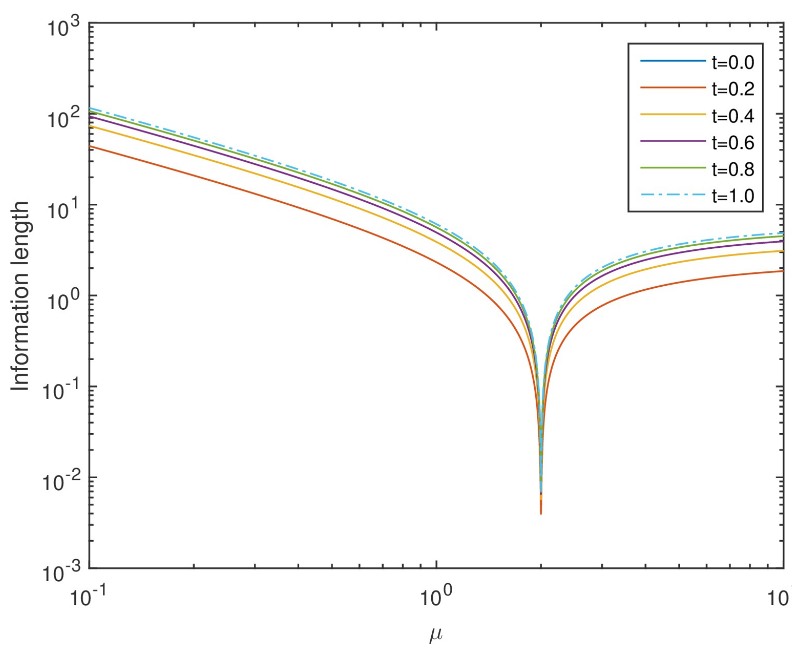

FIG. 3: $\mathcal{L}$ against μ shown at different t: $\beta_0 = 99$ and $\beta_* = 100$.

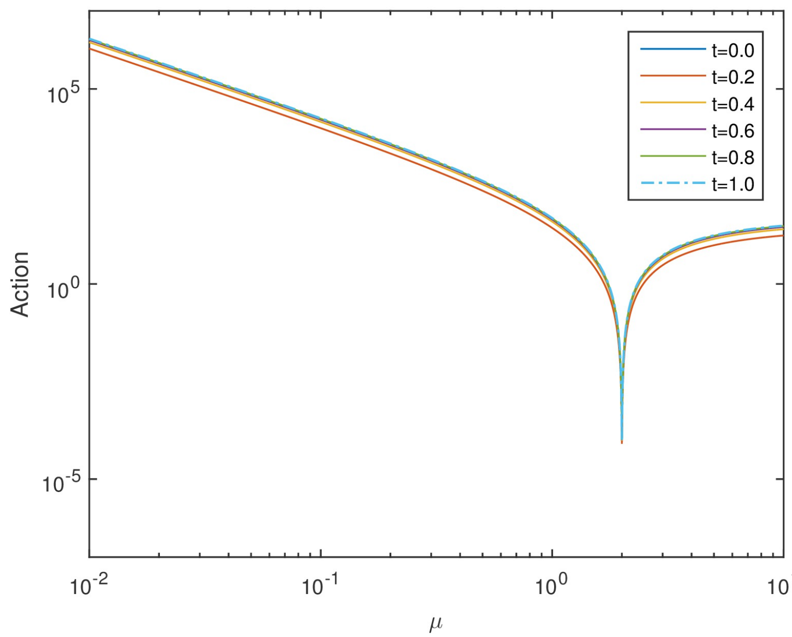

FIG. 4: $\mathcal{J}$ against μ shown at different t: $\beta_0 = 99$, $\beta_* = 100$.

and (22)), causing an artificial discontinuity due to the use of log scale on the y-axis. This is a clear reflection that $\mathcal{L}$ and $\mathcal{J}$ simply map all non-equilibrium states to their distance from this state. Interestingly, much similarity between panels (a) and (d) reveals that in either side of $\beta_0 = \beta_*$, the effect of changing the initial width of the PDF on the information length is quite similar whether it is narrower or wider than the equilibrium distribution. In particular, in all cases, we observe a similar power-law scaling for small μ ($< \mu_* = 2$), as can be seen by an almost straight line in the log-log plot of Figs. 5, as noted previously. Specifically, the gradient of the power-law scaling region in Figs. 3 and 5 are found to be approximately -1.0139 and -2.0403, respectively. That is, $\mathcal{L} \sim \frac{1}{\mu}$ and $\mathcal{J} \sim \frac{1}{\mu^2}$ [27].

Finally, we examine the variation in information velocity $\mathcal{J} - \frac{\mathcal{L}^2}{t}$ by using $u = 1$ in the following Cauchy-Schwartz inequality $\int_0^T v^2 \ dt \int_0^T u^2 dt \geq \left(\int_0^t v \ u \ dt \right)^2$. As is well known, the equality $\mathcal{J} = \mathcal{L}^2/t$ holds for the minimum path where v is constant (e.g. [21, 24, 25]), and the derivation from this equality quantifies the amount of disorder in an irreversable process [24], or deviation from a geodesic. To examine this variation, it is useful to consider the mean value of v obtained by time average $\langle v \rangle = \frac{1}{t} \int_0^t dt \ v$. By expressing $\mathcal{L}$ and $\mathcal{J}$ in

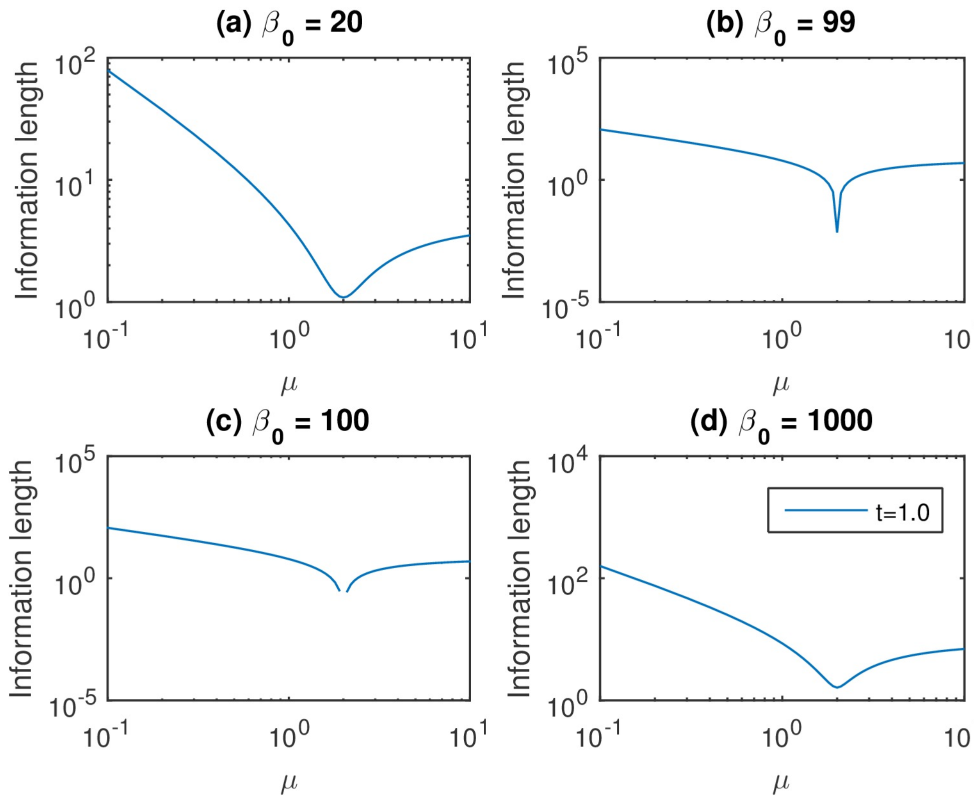

FIG. 5: $\mathcal{L}$ against μ for $\beta_0 = 20, 99, 100, 1000$ in (a)-(d): $\beta_0 = \beta_* = 100$ in panel (c).

terms of time averages, we express

$$\frac{\mathcal{J}}{t} - \frac{\mathcal{L}^2}{t^2} = \langle v^2 \rangle - \langle v \rangle^2 = \langle (\Delta v)^2 \rangle, \tag{23}$$

as a measure of the variation of the information velocity where $\Delta v = v - \langle v \rangle$. Fig. 6(a) shows $\mathcal{J} - \frac{\mathcal{L}^2}{t}$ against μ for different values of t for $\beta_0 = 90$ ($\beta_* = 100$). While $\mathcal{J} - \frac{\mathcal{L}^2}{t}$ monotonically increases with time, it takes its minimum at $\mu = 2$, with much larger value for $\mu < \mu_*$ than for $\mu > \mu_*$. However, associated with large $\mathcal{J} - \frac{\mathcal{L}^2}{t}$ for $\mu < \mu_*$, there is much larger $\langle v \rangle$ in this region. In order to quantify the fraction of variation relative to the average value, we normalize Eq. (23) by $\langle v \rangle^2$ to obtain

$$\frac{\mathcal{J}t}{\mathcal{L}^2} - 1 = \frac{\langle (\Delta v)^2 \rangle}{\langle v \rangle^2} = \frac{\langle v^2 \rangle}{\langle v \rangle^2} - 1. \tag{24}$$

We show the normalized version of Fig. 6(a) in Fig. 6(b), which exhibits the different dependence on μ. Specifically, $\frac{\langle (\Delta v)^2 \rangle}{\langle v \rangle^2}$ takes similar values near μ_* where it takes a maximum.

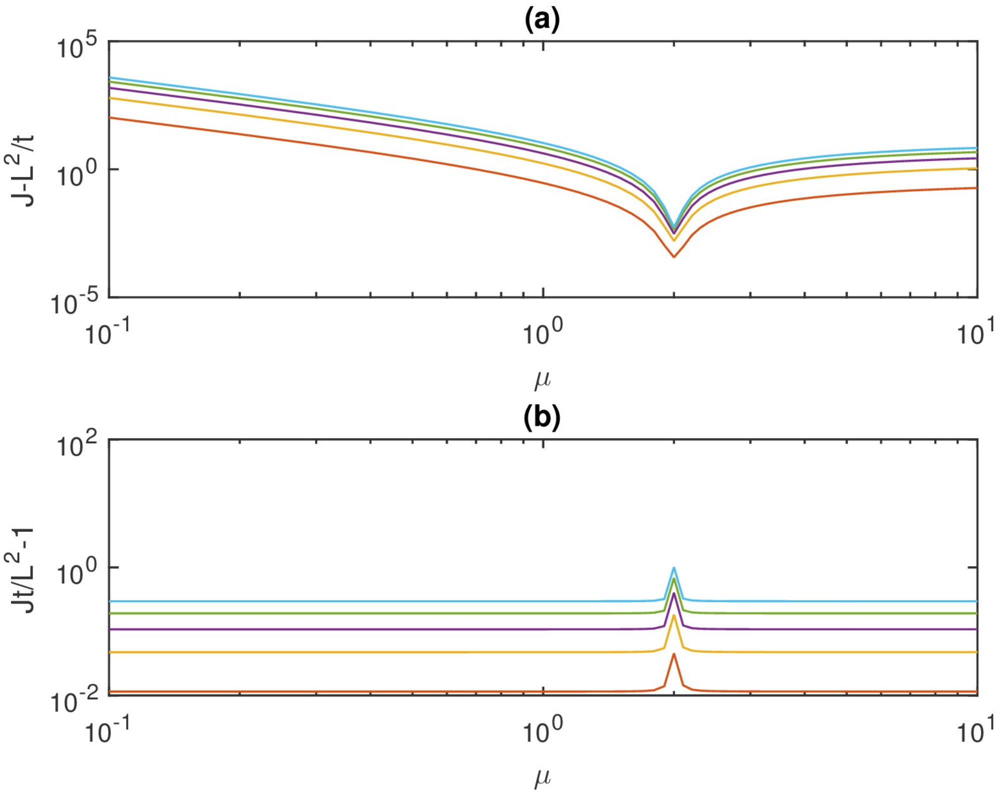

FIG. 6: (a) unnormalized Δv, (b) normalized Δv against μ for $\beta_0 = 90$

This suggets that *normalized* disorder quantified $\frac{\langle(\Delta v)^2\rangle}{\langle v\rangle^2}$ is largest around μ_* where $\mathcal{L}$ itself is smallest. For $\beta_0 \neq \beta_*$, $\frac{\langle(\Delta v)^2\rangle}{\langle v\rangle^2}$ tends to be larger for $\mu > \mu_*$ than for $\mu < \mu_*$ (figure not shown here). Fig. 7 shows $\mathcal{J} - \frac{\mathcal{L}^2}{t}$ and its normalized form given by Eq. (24) against t for $\beta_0 = \beta_*$. Interestingly, we can see that different lines in Panel (a) collapse into a single line in Panel (b) when scaled by the average information [28]. We note that this scaling is no longer valid for $r \neq 0$ (figure not shown here).

V. CONCLUSION

In order to measure the distance between two points in the cartesian coordinates, we use a uniform ruler as the unit of the distance. By generalizing this to non-equilibrium systems, we proposed a dynamical ruler whose resolution is set by time-dependent fluctuations associated

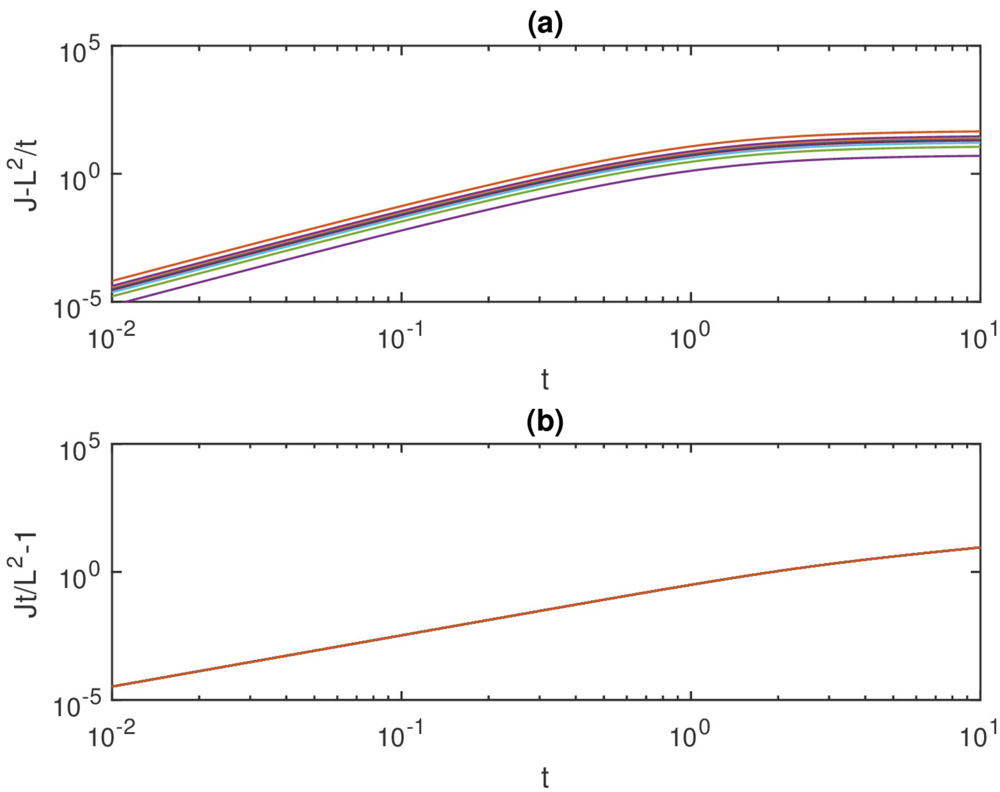

FIG. 7: (a) unnormalized Δv, (b) normalized Δv against t for $\beta_0 = 100$

with information change and mapped the evolution of a non-equilibrium system into a trajectory in a generalized metric space, where the distance between two points along the trajectory quantifies the change in information. The proposed mapping relation successfully captured not only the structure of attractor but also correlation between different non-equilibrium states. For our stochastic model with a multiplicative noise, we showed that the regions of $\mu > \mu_*$ is much closer to the equilibrium state μ_* than the region $\mu < \mu_*$. This suggests that the growth of population towards the equilibrium μ_* would require more information change compared to the decrease in population starting from large value ($\mu > \mu_*$) towards μ_*. For instance, the growth of a tumour to size μ_* would need more information change than that for the treatment of large-tumor to size μ_*. However, as one of the main characteristics of a tumor is a heavy-tail PDF for rare events of large size, the application of our work to tumours (or any other anomalous transport) would necessitate a different set of investigation by varying the final β_*; the application to tumour treatment would require the introduction of the effect of drug to our model where the optimal drug treatment schedule could be investigated by finding a geodesic. A close investigation into a geodesic is under progress at present [25]. Also, a mapping relation for more general attractors with multiple local minima and maxima would be of great interest in understanding the stability and transition among different states in the attractor, which will all be addressed in a future publication.

---

[1] A.P.L. Newton, E. Kim and H.-L. Liu, Phys. Plasmas, **20**, 092306 (2013).

[2] E. Kim, H. Liu and J. Anderson, Phys. Plasmas, **16**, 0552304 (2009).

[3] E. Kim and P.H. Diamond, Phys. Rev. Lett., **90**,185006 (2003).

[4] A.P. Feinberg and R.A. Irizarry, Proceedings of National Academy of Sciences of the United States of America, **107**, 1757 (2010).

[5] N.X. Wang, X.M. Zhang, X.B. Han, Braz. J. Phys., **42**, 253 (2012).

[6] J. Lee, J. Lee, K. S. Farquhar, J. Yun, C. Frankenberger, E. Bevilacqua, K. Yeung, E. Kim, G. Balázsi and M. R. Rosner, Proceedings of National Academy of Sciences of the United States of America, **111(3)**, E364 (2014).

[7] U. Lee, J.J. Skinner, J. Reinitz, M.R. Rosner, and E. Kim, PLoS One, **10**, e0132397 (2015).

[8] A. d'Onofrio, Chaos, Solitons, and Fractals, **41**, 875 (2009).

[9] H. Haken, Information and Self-organization: A macroscopic approach to complex systems, 3rd Ed., Springer, p.63-64 (2006).

[10] G. Ruppeiner, Phys. Rev. A., **20**, 1608 (1979).

[11] F. Schlögl, Z. Phys. B – Cond. Matt., **59**, 449 (1985).

[12] E.H. Feng and G.E. Crooks, Phys. Rev. E., **79**, 012104 (2009).

[13] W.K. Wootters, Phys. Rev. D, **23**, 357 (1981).

[14] S.L. Braunstein and C.M. Caves Phys. Rev. Lett., **72**, 3439 (1994).

[15] H. Strobel, W. Muessel, D. Linnemann, T. Zibold, D.B. Hume, L. Pezzé, A. Smerzi, M.K. Oberthaler, Science, **345**, 424 (2014).

[16] P. Salamon, J.D. Nulton and R.S. Berry, J. Chem. Phys., **82**, 2433 (1985).

[17] J. Nulton and P. Salamon and B Andresen and Qi Anmin, J Chem. Phys., **83**, 334 (1985).

[18] G.E. Crooks, Phys.l Rev. Lett., **99**, 100602 (2007).

[19] D.A. Sivak and G. E. Crooks Phys. Rev. Lett. **8**, 190602 (2012).

[20] L. Diósi, K. Kulacsy, B. Lukács and A. Rácz, J. Chem. Phys., **105**, 11220 (1996).

[21] P. Salamon. J.D. Nulton, G. Siragusa, A. Limon, D. Bedeaus and S. Kjelstrup, J. Non-Equilib. Thermodyn., **27**, 45 (2002).

[22] S.B. Nicholson and E. Kim, Phys. Lett. A., **379**, 8388 (2015)

[23] S.B. Nicholson and E. Kim, "Structures in sound: Analysis of Classical Music Using the Information Length, submitted to PLoS One (2015).

[24] S.W. Flynn, H.C. Zhao, and J.R. Green, J. Chem. Phys., **141**, 104107 (2014); J.W. Nichols, S.W. Flynn, J.R. Green, J. Chem. Phys., **142**, 064113 (2015).

[25] E. Kim and J. Heseltine, "Geometric structure and geodesic motion in a solvable model of non-equibrium stochastic process", in preparation (2015).

[26] Eq. (6) is valid when $P(x,t) \to 0$ as $x \to 0$

[27] This power-law dependence can be traced back to the form of the velocity square in Eq. (12) which becomes proportional to μ^{-2} for small μ as $q \propto 1/\mu^2$ as sufficiently small $\mu < 1$.

[28] We can easily check that $r = 0$, $\frac{(\Delta v)^2}{\langle v \rangle^2} \to \frac{\gamma t}{2} - 1$, which is independent of μ (See Fig. 7).